JACS
JOURNAL OF THE AMERICAN CHEMICAL SOCIETY
Communication
pubs.acs.org/JACS

Ultrathin Cobalt–Manganese Layered Double Hydroxide Is an Efficient Oxygen Evolution Catalyst

Fang Song and Xile Hu*

Laboratory of Inorganic Synthesis and Catalysis, Institute of Chemical Sciences and Engineering, Ecole Polytechnique Fédérale de Lausanne (EPFL), EPFL-ISIC-LSCI, BCH 3305, Lausanne, CH 1015, Switzerland

Supporting Information

ABSTRACT: Cost-effective production of solar fuels requires robust and earth-abundant oxygen evolution reaction (OER) catalysts. Herein, we report that ultrathin nanoplates of cobalt–manganese layered double hydroxide (CoMn LDH) are a highly active and stable oxygen evolution catalyst. The catalyst was fabricated by a one-pot coprecipitation method at room temperature, and its turnover frequency (TOF) is more than 20 times higher than the TOFs of Co and Mn oxides and hydroxides, and 9 times higher than the TOF of a precious IrO_2 catalyst. The activity of the catalyst was promoted by anodic conditioning, which was proposed to form amorphous regions and reactive Co(IV) species on the surface. The stability of the catalyst was demonstrated by continued electrolysis.

Water splitting offers an attractive chemical method for renewable energy storage.[1] The oxidative half reaction of water splitting, the oxygen evolution reaction (OER), is kinetically sluggish and leads to significant overpotential and energy loss.[2] Precious-metal electrocatalysts such as IrO_2 and RuO_2 are good OER catalysts, but their low abundance and high cost prohibit a large-scale application. Therefore, there is tremendous interest in developing inexpensive and earth-abundant OER catalysts.[3] In neutral and weakly basic solutions Co-phosphate and Ni-borate catalysts are efficient but still require about 400 mV overpotential to reach 10 mA cm^{-2}.[4] In alkaline solutions several forms of $NiFeO_x$ and perovskite $Ba_{0.5}Sr_{0.5}Co_{0.8}Fe_{0.2}O_{3-\delta}$ (BSCF) are even more active than IrO_2 and RuO_2, reaching 10 mA cm^{-2} below 300 mV overpotential.[5] It was proposed that the active form of $NiFeO_x$ catalyst has a layered structure.[6] In agreement with this hypothesis, NiFe layered double hydroxide (NiFe LDH) is a very active OER catalyst in basic solutions, and its activity can be further enhanced by coupling to a carbon nanotube or by exfoliation.[7] Many Co and Mn oxides including Co-containing LDHs such as NiCo and CoCo LDHs were studied for OER as well;[6,8] however, they are generally less active than IrO_2 and RuO_2. To expand the scope of nonprecious OER catalysts, more active Co and Mn-based oxides are desirable. Herein we report that the one-pot synthesized ultrathin nanoplates of cobalt–manganese LDH (CoMn LDH) are a highly active and stable catalyst for OER. The CoMn LDH catalyst exhibits much higher intrinsic activity than Co and Mn oxides, CoCo and NiCo LDHs, and IrO_2 nanoparticles.

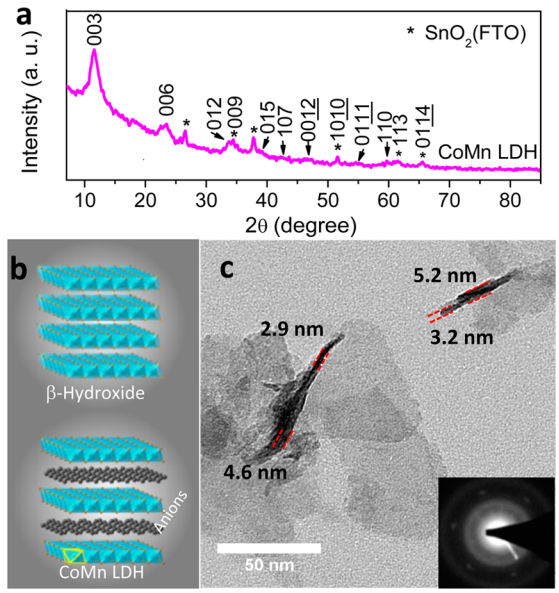

Figure 1. (a) PXRD pattern of CoMn LDH. Asterisks denote peaks from fluorine-doped SnO_2 glasses (JCPDS card No. 00-046-1088), which is the substrate for XRD measurement. (b) Structures of β-$Co(OH)_2$ and CoMn LDH. (c) TEM image of CoMn LDH nanoplates. Parallel red short dash lines mark the thickness of upstanding nanoplates. The inset shows the SAED pattern of a lying nanoplate along the [00n] axis.

The CoMn LDH nanoplates were synthesized at room temperature by a simple coprecipitation method. An aqueous solution containing $Co(NO_3)_2{\cdot}6H_2O$, $Mn(NO_3)_2{\cdot}4H_2O$, $NaNO_3$, and NH_4F was purged by N_2, and then H_2O_2 was added to oxidize Mn(II) to Mn(III). The pH was adjusted to about 10 by dropwise addition of a N_2-purged NaOH solution (see Supporting Information (SI) for details). The CoMn LDH was formed as an earthy yellow precipitate. The X-ray diffraction (XRD) pattern (Figure 1a) confirmed the LDH structure of the compound.[9] Figure 1b compares the atomic arrangement of CoMn LDH and β-$Co(OH)_2$. Replacement of some Co(II) ions in β-$Co(OH)_2$ by Mn(III) yields CoMn LDH. To compensate the extra positive charge, an equivalent amount of anion is intercalated between the edge-sharing MO_6 (M = Co or Mn) octahedral layers. This results in the layered structure of CoMn LDH (Figure 1b). Estimated from the angles of the XRD peaks,

Received: September 18, 2014
Published: November 7, 2014

   dx.doi.org/10.1021/ja5096733 | J. Am. Chem. Soc. 2014, 136, 16481–16484

the interlayer distance is about 0.759 nm for CoMn LDH. The energy-dispersive X-ray spectrum (EDX, Figure S1, SI) confirmed the presence of Co and Mn. The atomic ratios of Co/Mn in the as-synthesized samples were determined by inductively coupled plasma atomic emission spectroscopy (ICP-AES, Table S1, SI). The Co/Mn ratios are close to the ratios of Co/Mn in the starting materials and can be varied from 1:1 to 4:1. X-ray photoelectron spectroscopy (XPS, Figure S2, SI) suggests that Co and Mn ions are mainly in oxidation states Co(II) and Mn(III), respectively. Transmission electron microscopy (TEM) image indicates that the CoMn LDH has a platelet-like shape, with a diameter of 50−100 nm (Figure 1c). The near transparency to the electron beams (reflected by a faint image contrast) is indicative of the ultrathin nature. The thickness distribution was examined by measuring 153 upstanding platelets using TEM (Figure S3, SI). The average thickness is 3.6 nm, corresponding to six edge-sharing octahedral MO_6 layers. The selected area electron diffraction (SAED) pattern (inset in Figure 1c) was measured from one lying platelet. The hexagonally arranged spots indicate the single crystal nature of the platelet.

The electrochemical activity of CoMn LDH (Co/Mn = 2:1) and reference samples in OER in alkaline solutions was evaluated in 1 M KOH using a standard three-electrode system. Catalysts were uniformly drop-casted on a glassy carbon (GC) electrode with a loading of 0.142 mg cm^{-2}. After electrochemical conditioning by 30 cyclic voltammetric scans to reach a relatively stable state, the OER activity was probed by linear sweep voltammetry (LSV) at a scan rate of 1 mV s^{-1}. The reference samples include a mechanical mixture of $Co(OH)_2$ and Mn_2O_3 (see SI for synthesis, Figure S4), nonstoichiometric spinel $MnCo_2O_{4+\delta}$ ($0 < \delta < 0.5$, synthesized by calcinating CoMn LDH at 450 °C for 4 h, Figure S5, SI), and commercial IrO_2 nanoparticles (Figure S6, SI). Spinel $MnCo_2O_{4+\delta}$ was included as a reference because spinel Co-based metal oxides were previously reported as good OER catalysts in alkaline media.[8a,d,10] Figure 2a shows that CoMn LDH is the best OER catalyst among the samples measured, giving higher current densities at the same overpotentials (Figure 2a). To reach J = 10 mA cm^{-2}, the as-prepared CoMn LDH requires 324 mV (Figure 2b), which is 44, 92, and 13 mV less than $Co(OH)_2$ + Mn_2O_3, spinel $MnCo_2O_{4+\delta}$, and IrO_2, respectively. The current density at η = 350 mV is 42.5 mA cm^{-2} for CoMn LDH, which is about 7.6, 22.5, and 2.8 times of the current densitiy of $Co(OH)_2$ + Mn_2O_3, spinel $MnCo_2O_{4+\delta}$, and IrO_2, respectively. By plotting overpotential (η) against log(J), the kinetic parameters of OER by the four catalysts were calculated (inset in Figure 2a). The Tafel slop of CoMn LDH is 43 mV dec^{-1}, lower than the Tafel slope of IrO_2 (49 mV dec^{-1}). The Tafel slopes of $Co(OH)_2$ + Mn_2O_3 and spinel $MnCo_2O_{4+\delta}$ are significantly higher (54 and 84 mV dec^{-1}). While Tafel slopes might be used to probe the mechanism of OER catalysis,[2] they are often influenced by electron and mass transport. To test whether mass transport plays a role in OER, the scan rate dependence of the activity of CoMn LDH and $Co(OH)_2$ + Mn_2O_3 was measured. Increasing the scan rate from 2 to 5 mV/s led to negligible change in activity, suggesting that mass transport was sufficiently rapid (Figure S7, SI).[11] We recently showed that slow electron transport gave larger Tafel slopes for hydrogen evolution catalyzed by amorphous molybdenum sulfide particles.[12] Thus, the lower Tafel slope of CoMn LDH is likely due to faster electron transport on these ultrathin nanoplates. The four catalysts were also deposited on pretreated carbon fiber paper (CFP) at a loading of 0.222 mg

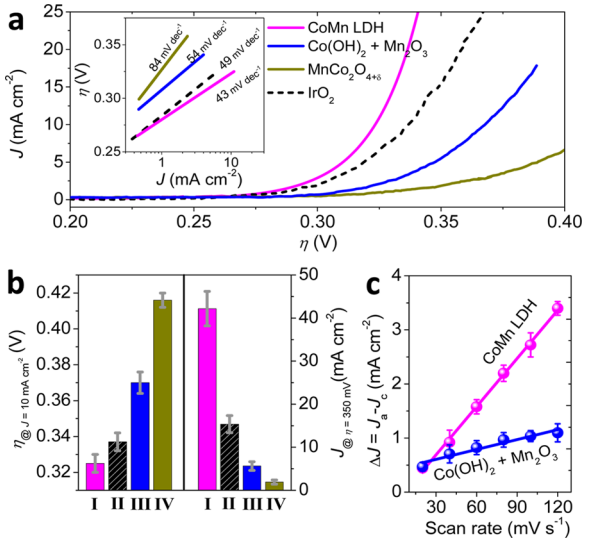

Figure 2. (a) Linear sweep voltammetric curves of various metal oxides in 1 M KOH; scan rate, 1 mV s^{-1}; scan direction, from lower to higher potentials. The inset showed corresponding Tafel plots. (b) Overpotential required for J = 10 mA cm^{-2} ($\eta_{@J=10\ mA\ cm^{-2}}$) and current density at η = 350 mV ($J_{@\eta=350\ mV}$). **I**, **II**, **III**, and **IV** represent CoMn LDH, IrO_2 nanoparticles, $Co(OH)_2$ + Mn_2O_3, and spinel $MnCo_2O_{4+\delta}$, respectively. (c) Charging current density differences ($\Delta J = J_a - J_c$) plotted against scan rates. The linear slope is equivalent to twice of the double-layer capacitance C_{dl}. The error bar represents the range of results from three independent measurements.

cm^{-2}, and the resulting electrodes show similar activity as on GC (Figure S8, SI). The Co/Mn ratio in CoMn LDH was tuned from 1:1, 2:1, and 3:1, to 4:1 by changing the Co/Mn ratio of the starting materials. The lowest activity was obtained with a ratio of 1:1, while the highest activity was obtained with a Co/Mn ratio of 2:1. Further increase in Co/Mn ratio then decreased the activity although only by a modest amount (Table S1 and Figure S9, SI).

The electrochemically active surface areas of CoMn LDH and $Co(OH)_2$ + Mn_2O_3 were compared using their double-layer capacitance (C_{dl}, Figure S10, SI).[13] Because of the similar structures and compositions of CoMn LDH and $Co(OH)_2$ + Mn_2O_3, C_{dl} is a reasonable parameter to represent their active surface areas. Figure 2c shows that CoMn LDH has a 5-times higher C_{dl} than $Co(OH)_2$ + Mn_2O_3. The 5-time higher effective surface area at the same loading contributed to the higher activity of CoMn LDH relative to $Co(OH)_2$ + Mn_2O_3. However, the increase in electrochemical surface area is not the sole factor for activity enhancement. For example, at η = 350 mV the current density of CoMn LDH is 7.6 times higher than that of $Co(OH)_2$ + Mn_2O_3 (Figure 2b). This was further confirmed by measuring the loading dependence of the OER activity of CoMn LDH and $Co(OH)_2$ + Mn_2O_3 on CFP. For both catalysts, a linear correlation of $J_{@\eta=350\ mV}$ and C_{dl} was found (Figure S11, SI). When the surface area factor is corrected, the CoMn LDH is still 2.2 time more active than $Co(OH)_2$ + Mn_2O_3. We attribute this activity enhancement to better charge transfer kinetics on CoMn LDH.

Interestingly, the OER activity of CoMn LDH can be significantly improved by anodic conditioning (AC). After 3 h of galvanostatic conditioning at an anodic current density J = 10 mA cm^{-2} (inset in Figure 3a), the overpotential ($\eta_{@J=10\ mA\ cm^{-2}}$) decreased by about 20 mV for CoMn LDH, but only negligibly (3 mV) for $Co(OH)_2$ + Mn_2O_3 (Figures 3a and S12, SI). AC for 17 h further decreased $\eta_{@J=10\ mA\ cm^{-2}}$ by 12 mV to 293 mV (Figure

dx.doi.org/10.1021/ja5096733 | J. Am. Chem. Soc. 2014, 136, 16481−16484

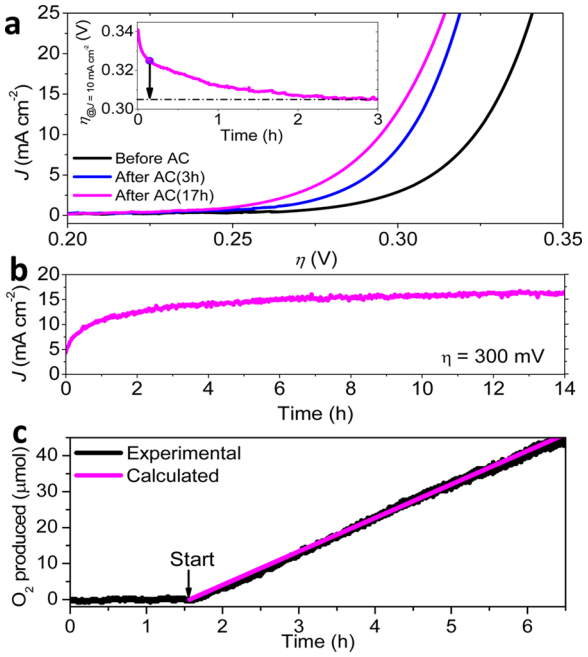

Figure 3. (a) LSV curves showing the effect of continuous anodic conditioning (AC) at J = 10 mA cm^{-2} for CoMn LDH. (b) Chronoamperometric curve at η = 300 mV for OER catalyzed by CoMn LDH for 14 h. (c) Calculated versus actual oxygen production catalyzed by CoMn LDH at a constant oxidative current of 1 mA.

3a). After this treatment, the current density reached 16.5 mA cm^{-2} at η = 300 mV, and 231 mA cm^{-2} at η = 350 mV. This enhanced activity is durable: the current density remained at 16.5 mA cm^{-2} at η = 300 mV for more than 10 h (Figure 3b). Figure S13, SI, shows that the high activity is maintained for more than 25 h in galvanostatic electrolysis. For comparison, the same 3 h AC increased the overpotential required for J = 10 mA cm^{-2} by 12 mV for IrO_2 nanoparticles (Figure S14, SI). These results indicate that the activity enhancement by AC is unique to CoMn LDH. The Faradaic efficiency for OER catalyzed by CoMn LDH was determined using a fluorescence O_2 detector. The Faradaic yield was quantitative during a 5 h electrolysis experiment (Figure 3c).

Table 1 compares the activity of CoMn LDH with Co−Pi, CoO_x, MnO_x, and their composites, as well as several state-of-the-art oxide catalysts including IrO_2, BSCF, CoCo and NiCo LDH, and $NiFeO_x$. To compare the intrinsic activity, turnover frequencies (TOFs) were used. The TOF of CoMn LDH was calculated assuming all the Co ions were active, which was the lower limit of the activity. The TOF of CoMn LDH at η = 350 mV (1.05 s^{-1}) was more than 20 times higher than those of Co−Pi, CoO_x, MnO_x, and their composites (such as mixed Co/Mn spinel), and nine times higher than that of IrO_2.[6,8a−e,10,14] This makes CoMn LDH the most active Co- or Mn-based OER catalyst to date. Bell and co-worker reported a higher TOF for a submonolayer CoO_x film deposited on Au.[15] However, the high activity of monolayer CoOx@Au was largely due to a strong promotion of Au, and the activity decreased dramatically when the loading was increased to 87 monolayers (~0.006 mg cm^{-2}). The activity of CoMn LDH is much higher than both bulk and exfoliated CoCo and NiCo LDH, highlighting the important influence of Mn. Table 1 also shows that the activity of CoMn LDH is comparable to the activity of the best $NiFeO_x$ and perovskite catalysts.[5c,6,7]

Table 1. Comparison of OER Activity in Alkaline Medium

Catalysts		TOFs (10^{-2} s^{-1})		Mass activity
		@350 mV	@300 mV	@300 mV (A g^{-1})
CoMn LDH[a,b]	After AC	105	7.5	159
	Before AC	13	0.9	18.8
Co/+Mn based (hydro) oxides	CoO_x[6,8a,b,8e,10]	0.08~5[b]	/	/
	MnO_x[6,8c,14a,14d]	0.02~2[c]	/	/
	$CoMnO_x$[8d,14b,g]	0.08~4[b]	/	/
	Co-Pi[4a]	~0.2[b,f]	/	/
CoO_x@Au[b]	~87 Monolayers[15]	6	/	/
	0.4 Monolayers[15]	180	/	/
CoCo LDH[b]	Bulk[7b]	/	0.14	/
	Exfoliated[7b]	/	0.35	/
NiCo LDH[b]	Bulk[7b]	/	0.32	/
	Exfoliated[7b]	/	1.1	/
$NiFeO_x$[d]	$NiFeO_x$[6]	/	21	/
	NiFe LDH[7a]	/	~4.9	/
	NiFe LDH @CNT[7a]	/	56	/
Perovskite[b]	BSCF[5c]	/	~0.71	~10
IrO_2[e]	Nanoparticles[6,14c,h]	/	0.6~0.8	11~15

[a]This work. Assuming all the following atoms are active for OER:. [b]Co, [c]Mn, [d]Ni, and [e]Ir atoms. [f]Caculated at η = 410 mV in pH = 7. [g]$Co(OH)_2$ + Mn_2O_3 and spinel $MnCo_2O_{4+\delta}$. [h]IrO_2 in this work.

The origin of the activity enhancement by AC was probed. The electrochemical surface area (determined by capacitance measurements) and the Tafel slopes of CoMn LDH are similar before and after AC (Figure S15, SI). Postcatalysis characterization of CoMn LDH after different AC intervals was then conducted. SEM, TEM, and XRD show that the nanoplate shape, crystal structure, and phase of CoMn LDH do not change during the AC process (Figures S16 and S17, SI), while HR-TEM reveals thin amorphous regions at the surface of the nanoplates of CoMn LDH after AC (Figure S18, SI). The elemental analysis by ICP-AES (Table S2, SI) shows that in the first 3 h of AC the Co/Mn atomic ratio increased from 2.001 to 2.088, indicating the leaching of Mn ions into the electrolyte. Similar leaching phenomenon was observed for $LiCoPO_4$ during OER catalysis: P leached from the surface to create amorphous surface phase, which was more active than crystalline $LiCoPO_4$.[16] We hypothesized that during AC, some Mn ions of CoMn LDH were leached at the surface to give amorphous layers. These amorphous regions (Figures S18 and S19, SI) are rich in under-coordinated Co ions (defect sites), which could be a factor for the enhanced activity after AC. Previously it was proposed that the key step for OER by CoO_x was the proton-coupled one-electron oxidation of Co^{III}−OH to Co^{IV}−O.[4b,15,17] It is possible that AC also leads to the accumulation of Co(IV) species in the newly formed amorphous layer to enhance the OER activity. This hypothesis needs to be tested by advanced in situ spectroscopic studies. For the moment, we obtained only indirect support by comparing the effects of AC on two different electrode substrates, GC and CFP. GC might be considered inert, while

dx.doi.org/10.1021/ja5096733 | J. Am. Chem. Soc. 2014, 136, 16481−16484

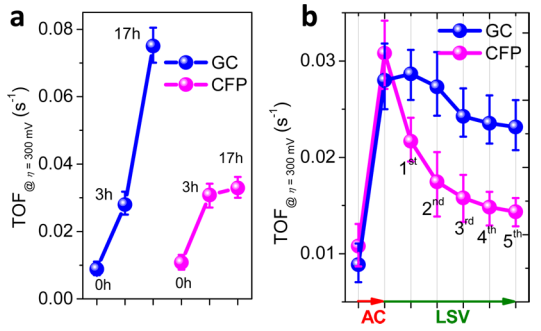

Figure 4. Comparisons of TOFs on GC and CFP at η = 300 mV. (a) Different AC time. (b) Degradation after AC (3 h). The error bar represents the range of results from three independent measurements.

CFP is more reductive. Figure 4a shows that CoMn LDH has similar activity on GC and CFP after 3 h of AC. However, further AC only increased the activity of the catalyst on GC; but not on CFP. This difference might be attributed to the reductive nature of CFP, which suppresses the accumulation of Co(IV). The OER activity of CoMn LDH after AC decreases when the anodic potential is removed (Figure S20, SI). This decay of activity is consistent with previous report that Co(IV) species only exist at operating potentials of OER.[15,17c−e,g] The decay of OER activity was examined by LSV (from 1.41 to 1.61 V vs RHE) after 3 h of AC (Figure S21, SI). Figure 3b shows that the decaying rate on CFP was much faster than the rate on GC. This is again consistent with the reductive nature of CFP.

In conclusion, we report that ultrathin nanoplates of CoMn LDH are a highly active and robust OER catalyst in alkaline medium. This is the first time that a Co- or Mn-based oxide exhibits comparable activity to the best Ni- or Fe-based oxide catalysts, which considerably expands the chemical space of earth-abundant OER catalysts. We uncover that anodic conditioning enhances significantly the activity of CoMn LDH catalyst, and we propose that this is due to the formation of amorphous layers at the surface and possibly the accumulation of active Co(IV) species in the amorphous layers.

■ ASSOCIATED CONTENT

Supporting Information

Experimental details and supporting data. This material is available free of charge via the Internet at http://pubs.acs.org.

■ AUTHOR INFORMATION

Corresponding Author

*xile.hu@epfl.ch.

Notes

The authors declare no competing financial interest.

■ ACKNOWLEDGMENTS

This work is supported by the EPFL. We thank Dr. Kurt Schenk (EPFL) for help with XRD and the Interdisciplinary Center for Electron Microscopy at EPFL for assistance in electron microscopic and XPS measurements.

■ REFERENCES

(1) Lewis, N. S.; Nocera, D. G. *Proc. Natl. Acad. Sci. U.S.A.* **2006**, *103*, 15729.

(2) Dau, H.; Limberg, C.; Reier, T.; Risch, M.; Roggan, S.; Strasser, P. *ChemCatChem* **2010**, *2*, 724.

(3) (a) Hocking, R. K.; Brimblecombe, R.; Chang, L. Y.; Singh, A.; Cheah, M. H.; Glover, C.; Casey, W. H.; Spiccia, L. *Nat. Chem.* **2011**, *3*, 461. (b) Subbaraman, R.; Tripkovic, D.; Chang, K. C.; Strmcnik, D.; Paulikas, A. P.; Hirunsit, P.; Chan, M.; Greeley, J.; Stamenkovic, V.; Markovic, N. M. *Nat. Mater.* **2012**, *11*, 550. (c) Smith, R. D. L.; Prevot, M. S.; Fagan, R. D.; Zhang, Z. P.; Sedach, P. A.; Siu, M. K. J.; Trudel, S.; Berlinguette, C. P. *Science* **2013**, *340*, 60. (d) Indra, A.; Menezes, P. W.; Zaharieva, I.; Baktash, E.; Pfrommer, J.; Schwarze, M.; Dau, H.; Driess, M. *Angew. Chem., Int. Ed.* **2013**, *52*, 13206. (e) Gorlin, Y.; Lassalle-Kaiser, B.; Benck, J. D.; Gul, S.; Webb, S. M.; Yachandra, V. K.; Yano, J.; Jaramillo, T. F. *J. Am. Chem. Soc.* **2013**, *135*, 8525.

(4) (a) Kanan, M. W.; Nocera, D. G. *Science* **2008**, *321*, 1072. (b) Kanan, M. W.; Yano, J.; Surendranath, Y.; Dinca, M.; Yachandra, V. K.; Nocera, D. G. *J. Am. Chem. Soc.* **2010**, *132*, 13692.

(5) (a) Louie, M. W.; Bell, A. T. *J. Am. Chem. Soc.* **2013**, *135*, 12329. (b) Kuai, L.; Geng, J.; Chen, C. Y.; Kan, E. J.; Liu, Y. D.; Wang, Q.; Geng, B. Y. *Angew. Chem., Int. Ed.* **2014**, *53*, 7547. (c) Suntivich, J.; May, K. J.; Gasteiger, H. A.; Goodenough, J. B.; Shao-Horn, Y. *Science* **2011**, *334*, 1383.

(6) Trotochaud, L.; Ranney, J. K.; Williams, K. N.; Boettcher, S. W. *J. Am. Chem. Soc.* **2012**, *134*, 17253.

(7) (a) Gong, M.; Li, Y. G.; Wang, H. L.; Liang, Y. Y.; Wu, J. Z.; Zhou, J. G.; Wang, J.; Regier, T.; Wei, F.; Dai, H. J. *J. Am. Chem. Soc.* **2013**, *135*, 8452. (b) Song, F.; Hu, X. L. *Nat. Commun.* **2014**, *5*, 4477.

(8) (a) Esswein, A. J.; McMurdo, M. J.; Ross, P. N.; Bell, A. T.; Tilley, T. D. *J. Phys. Chem. C* **2009**, *113*, 15068. (b) Lu, Z.; Wang, H.; Kong, D.; Yan, K.; Hsu, P.-C.; Zheng, G.; Yao, H.; Liang, Z.; Sun, X.; Cui, Y. *Nat. Commun.* **2014**, *5*, 4345. (c) Fekete, M.; Hocking, R. K.; Chang, S. L. Y.; Italiano, C.; Patti, A. F.; Arena, F.; Spicci, L. *Energy Environ. Sci.* **2013**, *6*, 2222. (d) Cheng, F. Y.; Shen, J. A.; Peng, B.; Pan, Y. D.; Tao, Z. L.; Chen, J. *Nat. Chem.* **2011**, *3*, 79. (e) Zou, X.; Goswami, A.; Asefa, T. *J. Am. Chem. Soc.* **2013**, *135*, 17242. (f) Lin, H.; Zhang, Y.; Wang, G.; Li, J. B. *Front. Mater. Sci.* **2012**, *6*, 142. (g) Zhang, Y.; Cui, B.; Zhao, C. S.; Lin, H.; Li, J. B. *Phys. Chem. Chem. Phys.* **2013**, *15*, 7363.

(9) Zhao, J. W.; Chen, J. L.; Xu, S. M.; Shao, M. F.; Yan, D. P.; Wei, M.; Evans, D. G.; Duan, X. *J. Mater. Chem. A* **2013**, *1*, 8836.

(10) (a) Maiyalagan, T.; Jarvis, K. A.; Therese, S.; Ferreira, P. J.; Manthiram, A. *Nat. Commun.* **2014**, *5*, 3949. (b) Chou, N. H.; Ross, P. N.; Bell, A. T.; Tilley, T. D. *ChemSusChem* **2011**, *4*, 1566. (c) Sun, Y.; Gao, S.; Lei, F.; Liu, J.; Liang, L.; Xie, Y. *Chem. Sci.* **2014**, *5*, 3976. (d) Jiao, F.; Frei, H. *Energy Environ. Sci.* **2010**, *3*, 1018.

(11) Ma, T. Y.; Dai, S.; Jaroniec, M.; Qiao, S. Z. *Angew. Chem., Int. Ed.* **2014**, *53*, 7281.

(12) Vrubel, H.; Moehl, T.; Gratzel, M.; Hu, X. L. *Chem. Commun.* **2013**, *49*, 8985.

(13) Merki, D.; Vrubel, H.; Rovelli, L.; Fierro, S.; Hu, X. L. *Chem. Sci.* **2012**, *3*, 2515.

(14) (a) Meng, Y.; Song, W.; Huang, H.; Ren, Z.; Chen, S.-Y.; Suib, S. L. *J. Am. Chem. Soc.* **2014**, *136*, 11452. (b) Gao, M. R.; Xu, Y. F.; Jiang, J.; Zheng, Y. R.; Yu, S. H. *J. Am. Chem. Soc.* **2012**, *134*, 2930. (c) Lee, Y.; Suntivich, J.; May, K. J.; Perry, E. E.; Shao-Horn, Y. *J. Phys. Chem. Lett.* **2012**, *3*, 399. (d) Gorlin, Y.; Chung, C. J.; Benck, J. D.; Nordlund, D.; Seitz, L.; Weng, T. C.; Sokaras, D.; Clemens, B. M.; Jaramillo, T. F. *J. Am. Chem. Soc.* **2014**, *136*, 4920.

(15) Yeo, B. S.; Bell, A. T. *J. Am. Chem. Soc.* **2011**, *133*, 5587.

(16) Lee, S. W.; Carlton, C.; Risch, M.; Surendranath, Y.; Chen, S.; Furutsuki, S.; Yamada, A.; Nocera, D. G.; Shao-Horn, Y. *J. Am. Chem. Soc.* **2012**, *134*, 16959.

(17) (a) Brunschwig, B. S.; Chou, M. H.; Creutz, C.; Ghosh, P.; Sutin, N. *J. Am. Chem. Soc.* **1983**, *105*, 4832. (b) Singh, R. N.; Koenig, J. F.; Poillerat, G.; Chartier, P. *J. Electrochem. Soc.* **1990**, *137*, 1408. (c) Lyons, M. E. G.; Brandon, M. P. *Int. J. Electrochem. Sci.* **2008**, *3*, 1425. (d) McAlpin, J. G.; Surendranath, Y.; Dinca, M.; Stich, T. A.; Stoian, S. A.; Casey, W. H.; Nocera, D. G.; Britt, R. D. *J. Am. Chem. Soc.* **2010**, *132*, 6882. (e) Surendranath, Y.; Kanan, M. W.; Nocera, D. G. *J. Am. Chem. Soc.* **2010**, *132*, 16501. (f) Wasylenko, D. J.; Ganesamoorthy, C.; Borau-Garcia, J.; Berlinguette, C. P. *Chem. Commun.* **2011**, *47*, 4249. (g) Doyle, R. L.; Godwin, I. J.; Brandon, M. P.; Lyons, M. E. G. *Phys. Chem. Chem. Phys.* **2013**, *15*, 13737.